

Two-step Dimerization for Autoproteolysis to Activate Glycosylasparaginase*

Received for publication, October 11, 2002, and in revised form, November 10, 2002
Published, JBC Papers in Press, November 13, 2002, DOI 10.1074/jbc.M210431200

Yeming Wang and Hwai-Chen Guo‡

From the Department of Physiology and Biophysics, Boston University School of Medicine,
Boston, Massachusetts 02118-2526

Glycosylasparaginase (GA) is an amidase and belongs to a novel family of N-terminal nucleophile hydrolases that use a similar autoproteolytic processing mechanism to generate a mature/active enzyme from a single chain protein precursor. From bacteria to eukaryotes, GAs are conserved in primary sequences, tertiary structures, and activation of amidase activity by intramolecular autoproteolysis. An evolutionarily conserved His-Asp-Thr sequence is cleaved to generate a newly exposed N-terminal threonine, which plays a central role in both autoproteolysis and in its amidase activity. We have recently determined the crystal structure of the bacterial GA precursor at 1.9-Å resolution, which reveals a highly distorted and energetically unfavorable conformation at the scissile peptide bond. A mechanism of autoproteolysis via an N-O acyl shift was proposed to relieve these conformational strains. However, it is not understood how the polypeptide chain distortion was generated and preserved during the folding of GA to trigger autoproteolysis. An obstacle to our understanding of GA autoproteolysis is the uncertainty concerning its quaternary structure in solution. Here we have revisited this question and show that GA forms dimers in solution. Mutants with alterations at the dimer interface cannot form dimers and are impaired in the autoproteolytic activation. This suggests that dimerization of GA plays an essential role in autoproteolysis to activate the amidase activity. Comparison of the melting temperatures of GA dimers before and after autoproteolysis suggests two states of dimerization in the process of enzyme maturation. A two-step dimerization mechanism to trigger autoproteolysis is proposed to accommodate the data presented here as well as those in the literature.

Glycosylasparaginase (GA)¹ is an amidase involved in Asn-linked glycoprotein degradation (1). A deficiency in the human GA leads to severe clinical symptoms, known as aspartylglycosaminuria (2). GA is widely distributed in vertebrate tissues (3), insect cells (4), and in bacteria (5). GA joins the proteasome

and penicillin acylase as a novel class of enzymes, called N-terminal nucleophile (Ntn) hydrolases that catalytically use a processed N-terminal threonine, serine, or cysteine as both a polarizing base and a nucleophile (6). The crystal structures of human and bacterial GA show a similar structural frame of an $\alpha\beta\alpha$ -sandwich, common to all the Ntn hydrolases (7–10). One intriguing aspect of GA is that a single chain precursor is processed by intramolecular autoproteolysis that generates the 17-kDa α - and 15-kDa β -subunits and exposes the active site threonine at the newly generated N-terminal end of the β -subunit (11, 12). A similar mechanism is utilized in protein splicing that involves two concerted autocleavages and one ligation of the polypeptide chain (13, 14).

Crystal structures of GA precursor have provided us a structural basis to propose a detailed mechanism of intramolecular autoproteolysis (15). The GA precursor undergoes a two-step mechanism to break up the polypeptide chain, through an N-O acyl shift and an ester intermediate. In the first step, the nucleophile Thr-152 is activated by a base Asp-151 that is held in an unusual but precise geometry by Thr-203 to deprotonate the nucleophile Thr-152. After the nucleophilic attack, a transitional tetrahedral anion intermediate is stabilized by a polar group of Thr-170 that could further be polarized to carry positive charge by Arg-180, possibly through a bound solvent molecule. Collapse of the tetrahedral anion intermediate shifts the linkage from an amide bond to an ester bond (N-O acyl shift). Usually the equilibrium of N-O acyl shift favors the amide bond, resulting in a peptide bond that does not break often at threonine, serine, or cysteine. However, the strained, tight turn conformation at the scissile peptide bond observed in the GA precursor structures could drive the equilibrium toward an ester bond formation (15). The second step of autoproteolysis is a simple hydrolysis of the ester intermediate by a neighboring water molecule, resulting in an active amidase with α - and β -subunits. Recently, both scissile peptide bonds involved in protein splicing of PI-SceI have also been found to be in distorted *trans* conformations (16). Similar to GA autoproteolysis, relieving the distorted/strained main chain atoms is also believed to help drive an N-S acyl shift in PI-SceI precursor.

It is not understood how the polypeptide chain distortion to trigger autoproteolysis is generated and why these local constraints are not removed during the folding of the GA precursor. It seems plausible that the structural constraints are generated only at a late stage of protein folding, for example, during the formation of the native quaternary structure. Dimerization of GA precursors has been suggested to be a prerequisite to trigger autoproteolysis (8, 17, 18). However, the native quaternary structure of GA was controversial. Among several crystal forms, the same dimer structure is observed for the human and bacterial GA, either as precursors or autoproteolyzed enzymes (7–9, 15). However, in solution, GA was reported as monomeric for mammalian and bacterial enzymes (3,

* This work was supported by United States Public Health Service Grant DK53893 from the NIDDK, National Institutes of Health. The costs of publication of this article were defrayed in part by the payment of page charges. This article must therefore be hereby marked "advertisement" in accordance with 18 U.S.C. Section 1734 solely to indicate this fact.

‡ To whom correspondence should be addressed: Dept. of Physiology and Biophysics, Boston University School of Medicine, 715 Albany St., Boston, MA 02118-2526. Tel.: 617-638-4023; Fax: 617-638-4041; E-mail: hguo@bu.edu.

¹ The abbreviations used are: GA, glycosylasparaginase; AGU, aspartylglycosaminuria; Ntn, N-terminal nucleophile; T152Cm, autoproteolyzed/mature form of the T152C mutant protein; MBP, maltose-binding protein; DMS, dimethyl sulfoxide; PI, protein intervening sequence.

9, 11, 19), whereas others reported dimeric GA for the human (17, 20), chicken (3), and insect enzymes (4).

This study was designed to re-examine the native quaternary structure of GA in solution and to study the significance of the quaternary structure in the intramolecular autoproteolysis that is essential to activate the amidase activity for glycoprotein degradation. By using biochemical and biophysical methods, we confirm that GA exists as dimers in solution. Structure-based mutants designed to disrupt the dimer interface lose their ability to form dimers and also lose their ability for autoproteolytic activation of amidase activity.

EXPERIMENTAL PROCEDURES

Protein Purification—Proteins were expressed and purified by existing procedures (21), with some modifications. The expression of maltose-binding protein (MBP)-GA fusion proteins was induced in the TB1 cells by adding 1 mM isopropyl-1-thio- β -D-galactopyranoside overnight at 30 °C. Cells were pelleted by centrifugation, resuspended in 20 mM Tris buffer, pH 7.6, 50 mM NaCl, 1 mM EDTA, and lysed by sonication. Fusion proteins were affinity-purified from the crude extracts over an amylose column according to the protocol of the manufacturer (New England Biolabs). All purification procedures were carried out at 4 °C. To obtain GA proteins, the purified fusion proteins were further digested with factor Xa at room temperature overnight, and GA was then separated from MBP and factor Xa with a HiTrap Q-Sepharose (Amersham Biosciences) column. Similar protocols were used to purify autoproteolysis-inactive mutant precursors (T152A). For the precursor proteins of autoproteolysis-active mutant precursors (T152C mutant), 10 mM glycine was included during the entire course of protein expression and purification to inhibit autoproteolysis. Protein concentration was determined by absorbance measurements at 280 nm in 6 M guanidine hydrochloride (22).

Gel Filtration—A 200- μ l volume, 20 μ M each of the GA or MBP fusion proteins, was applied to an Amersham Biosciences HiPrep 16/60 Sephacryl S-200 HR gel filtration column, equilibrated in a solution containing 10 mM potassium-phosphate buffer, pH 7.4, and 1 mM EDTA. According to the manufacturer, this column effectively separates globular proteins in the molecular mass range of 5–250 kDa. The gel filtration standards, a mixture of five molecular weight markers, were purchased from Bio-Rad: bovine thyroglobulin (670 kDa), bovine γ -globulin (158 kDa), chicken ovalbumin (44 kDa), equine myoglobin (17 kDa), and vitamin B-12 (1,350 Da). Thus, bovine thyroglobulin was eluted at the point representing the void volume of the column.

Cross-linking with Glutaraldehyde and DMS—Cross-linking was performed at 0.1–0.2 mg/ml (1.3–6.2 μ M) protein and 0.0005–1% glutaraldehyde in 10 mM potassium-phosphate buffer, pH 7.4, and incubation for 6 h at room temperature. Reactions were quenched with 0.15 volumes of 0.5 M glycine. Cross-linked protein samples were denatured in 1% SDS, 1% β -mercaptoethanol at 90 °C for 10 min, and then analyzed by SDS-PAGE. The gels were stained with Coomassie Blue. Similar experiments were also performed using 1–4 mg/ml dimethyl suberimidate (DMS) as a cross-linking reagent.

Sucrose Density Gradient Sedimentation—Sedimentation was performed using a modified version of the method described by Martin and Ames (23). Linear gradients of 10–30% sucrose in 10 mM potassium-phosphate buffer, pH 7.4, were equilibrated at 4 °C for 2–4 h prior to use. Protein was diluted in the same buffer to 30 μ M, preincubated for 30 min at 4 °C, and then layered on the gradients using a 20-gauge needle. Gradients were centrifuged 40,000 rpm for 12 h in a Beckman SW55 Ti rotor. Gradients were withdrawn from the top into a series of 100- μ l fractions. Protein peaks in the gradient were determined by Bradford assays of each fraction with reading of absorbance at 595 nm.

Site-directed Mutagenesis—DNA manipulation and site-directed mutagenesis (Kunkel methods) were carried out as described previously (11). Wild-type *Flavobacterium glycosylasparaginase* coding sequence was cloned into either the pMAL system or the Litmus system for site-directed mutagenesis, following the manufacturer's protocols (New England Biolabs). DNA clones with desired mutations were confirmed by sequence analyses using an ABI automatic DNA sequencer.

CD Spectrum Determination—CD spectra were recorded from 185 to 250 nm using an AVIV 62DS spectrometer equipped with a thermoelectric sample temperature controller, with a 1-mm path length cuvette. Protein concentrations were 2–5 μ M in 10 mM potassium-phosphate buffer, pH 7.4, and 1 mM EDTA and were determined by absorbance measurements in 6 M guanidine hydrochloride (22). The spectra were collected at 25 °C as the average of 10 scans, using a 15-s integration

time at 1.0 nm wavelength increments. Following the buffer base-line correction, the spectra were normalized to the protein concentration and are expressed as molar ellipticity.

Thermal Denaturation—Thermal unfolding curves were recorded at 222 nm upon heating from 5 to 95 °C at a rate of 60 °C/h, with a 1 °C increment, 30-s accumulation time. The melting temperature (T_m) was determined from the differential melting curves $d[\Theta_{222}]/dT$ (24). ORIGIN software (Microcal, Inc.) was used for the CD analyses and display.

RESULTS

GA Eluted as a Single Peak from Gel Filtration Column—Previous reports concerning the native GA quaternary structure drew conclusions mainly based on the apparent molecular masses on sizing chromatography or native gel electrophoresis, often using samples from cell extracts and visualizing a trace amount of GA by Western blot methods. Contradicting observations were reported from different groups; some concluded GA monomers (3, 9, 11, 19), whereas others reported dimers for GA precursor or autoproteolyzed GA (3, 4, 17, 20). These contradictory observations have prompted us to re-investigate the quaternary structure of GA more closely using purified precursors and the autoproteolyzed enzyme of *Flavobacterium* GA.

Wild-type GA spontaneously autoproteolyzes in cells into the mature form amidase with two (α and β) subunits, and thus it is impossible to isolate the precursor of wild-type GA. To study the quaternary structure of purified GA precursor, we thus have to resort to GA mutants. T152A precursor has the same three-dimensional structure as other precursor proteins that are active in autoproteolysis (15). Due to the loss of its critical nucleophile for autoproteolysis, we are able to purify a large quantity of precursor protein of the T152A mutant. Autoproteolysis of a second mutant, T152C, can be switched on and off by a reversible inhibitor, glycine (15). With the exception of a slower reaction rate, T152C resembles the wild-type GA in autoproteolysis activity (11, 25), and the autoproteolyzed T152C enzyme (T152Cm) has an identical crystal structure to that of the wild-type mature enzyme (8). Throughout this study, the T152A precursor was used to represent a native precursor structure, whereas the wild-type and/or mature T152Cm proteins were used to represent a native structure of mature GA amidase after autoproteolysis.

The purified GA proteins were first examined by chromatography on a gel filtration column. Because the native autoproteolyzed amidase still has the two newly generated (α and β) subunits in tight association (26, 27), a single chain GA precursor and a native autoproteolyzed amidase should have similar calculated molecular masses of 32 kDa. As shown in Fig. 1A, autoproteolyzed amidase of wild-type GA or T152Cm protein was eluted as a single peak with an apparent molecular mass of 43 kDa, when compared with a mixture of gel filtration size standards (Bio-Rad). Thus, the apparent molecular mass of mature GA was about 40% larger than a GA monomer of 32 kDa. Similarly, purified precursor T152A protein was eluted as a single peak with an apparent molecular mass of about 1.4-fold of a monomer. The precursor was eluted at a slightly larger volume than the mature enzyme. This is consistent with an uncleaved loop in the precursor that becomes cleaved and thus more floppy and bulky in the mature enzyme. Interestingly, a 43-kDa recombinant maltose-binding protein (MBP2 from New England Biolabs) was eluted with a substantially smaller apparent molecular mass (about 25 kDa) when compared with the same size standards (Fig. 1B). All these observations demonstrated the limitations of using gel filtration chromatography to estimate molecular masses of macromolecules, because the mobility of proteins in gel filtration columns was affected not only by molecular weight and size but also by molecular shape. There are various ways to interpret the single peaks of GA on chromatograms with elution volumes at the middle between

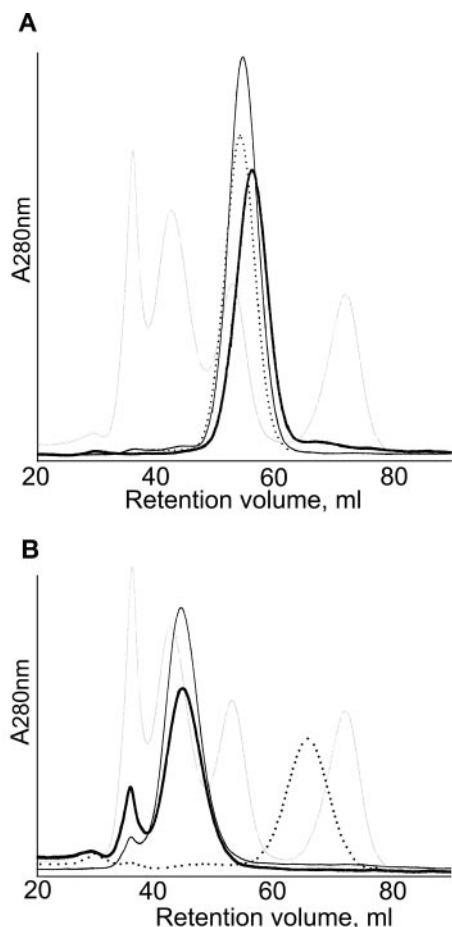


FIG. 1. Gel filtration chromatograms of GA and MBP-GA fusion proteins. *A*, purified GA proteins. *Dotted line*, autoprotoolyzed wild-type GA; *thin line*, autoprotoolyzed T152Cm protein; *thick line*, T152A precursor; and *background line*, a mixture of molecular mass standards from left to right: bovine thyroglobulin (670 kDa), bovine γ -globulin (158 kDa), chicken ovalbumin (44 kDa), and equine myoglobin (17 kDa). *B*, purified MBP-GA fusion proteins. *Dotted line*, MBP protein; *thin line*, autoprotoolyzed MBP-T152Cm protein; *thick line*, MBP-T152A precursor; and *background line*, the same molecular mass standards as in *a*. Proteins were gel-filtrated in a solution of 10 mM potassium-phosphate buffer, pH 7.4, and 1 mM EDTA, with a flow rate of 0.5 ml/min.

those expected for monomers and dimers. These single peaks could represent GA monomers with a smaller retention volume when compared with the size standards, which may be due to an extensive hydrophobic surface observed in the crystal structures. These single peaks could also be interpreted as GA dimers with a larger retention volume than expected, which may be due to the compact shape of the dimer observed in the crystal structures (8). A third explanation for the unusual mobility is that GA dimers are in fast equilibrium with monomers during the run through the gel filtration column. This uncertainty appears to be the source of confusion that results in contradictory reports in the literature.

MBP-GA Fusion Proteins Behave More Like Dimers on Gel Filtration Column—In an attempt to demonstrate the sensitivity of gel filtration chromatography to the shape of proteins, we re-examined the behavior of GA fusion proteins on the gel filtration column. We reasoned that attaching an MBP to the N-terminal end of GA protein would change the shape of a monomer from a quite compact GA structure to an irregular shape of a fusion protein. Therefore, if existing as a single species in solution, these fusion proteins might behave differently from GA protein alone and thus provide better resolution

to distinguish monomers from dimers. Otherwise, if GA dimers are in equilibrium with monomers, the fusion proteins would still be eluted as single peaks with apparent molecular masses of about 1.4-fold of a monomer.

Fig. 1*B* shows the gel filtration chromatograms for purified MBP-GA fusion proteins, before and after the GA domain was autoprotoolyzed. As a control, MBP protein alone was eluted as a single peak with an apparent molecular mass of 25 kDa, which is smaller than that calculated for a monomer of 43 kDa. Nonetheless, it indicates that MBP does not dimerize in solution. For a monomeric MBP-GA fusion protein, either as a precursor or an autoprotoolyzed amidase, the calculated molecular mass is 75 kDa. The MBP-T152A (GA precursor) fusion protein was eluted as a single peak, with an apparent molecular mass of 138 kDa. Likewise, MBP fusion with T152C mature GA (MBP-T152Cm) was eluted with an apparent molecular mass of 138 kDa that is 1.8-fold of the calculated molecular mass for a monomer. This shift of molecular mass from 1.4- to 1.8-fold of a monomer indicates that the unusual mobility of GA is not a result of fast equilibrium. Thus, considering that MBP alone was eluted at 0.6-fold of its calculated molecular weight, the MBP-GA fusion proteins eluted at 1.8-fold of the calculated molecular masses are more likely to be dimers than monomers. These results also suggest that the dimerization of fusion proteins is mediated by the GA domain and not the MBP domain.

GA Dimers Are Confirmed by Cross-linking Experiments—To confirm GA dimers in solution, we performed cross-linking with glutaraldehyde and DMS. Cross-linking of T152A precursor with 0.001–1% glutaraldehyde (amine-amine cross-linking) at room temperature and 0.1 mg/ml (3.1 μ M) protein indicated that the GA precursor was dimeric under these conditions (Fig. 2). Following SDS-PAGE, the T152A precursor yielded a characteristic pattern of two bands corresponding to cross-linked monomer and dimer (Fig. 2*A*), whereas an uncross-linked control (*i.e.* without glutaraldehyde treatment) gave a single band corresponding to a monomer. Similar cross-linking results were obtained with autoprotoolyzed enzyme of wild-type GA (Fig. 2*B*), although the pattern is more complicated because there are two subunits, α and β , in each native mature/autoprotoolyzed enzyme. Without cross-linking treatment, the wild-type mature enzyme gave two bands for the α - and β -subunits. A low dose of cross-linking reagent (0.001–0.01%) gave a new cluster of bands of 30–34 kDa corresponding to two cross-linked subunits either from the same GA molecule (α - β and α' - β' of 32 kDa) or through the dimer interface (α - α' , α - β' , α' - β , and β - β' ranging from 30 to 34 kDa). At higher concentrations of cross-linking treatment (0.1–1%), an additional cluster of bands was present corresponding to completely cross-linked dimer of autoprotoolyzed enzyme (~64 kDa of α - β - α' - β'). No band corresponding to three cross-linked subunits (*e.g.* α - β - α' , etc.) appeared. This might be due to a preferential cross-linking of contacts either through dimer interface or within a monomer. Thus, by the time two subunits were cross-linked through the minor cross-linking surface, they were also cross-linked through the major cross-linking surface, resulting in the 64-kDa species. The cross-linking pattern of mature T152Cm protein (Fig. 2*C*) is the same as the wild-type enzyme and confirms a dimeric structure of mature enzyme. Similar results were also obtained using DMS as the cross-linking reagent (data not shown). All together, results here confirm that both GA precursor and mature enzyme form dimers in solution.

Disruption of the Dimer Interface Prevents Both Autoprotoolysis and Dimer Formation—To examine the significance of dimerization in autoprotoolysis, we designed and generated mutants that would disrupt dimer interactions without affecting protein folding. With the aid of the crystal structures of the

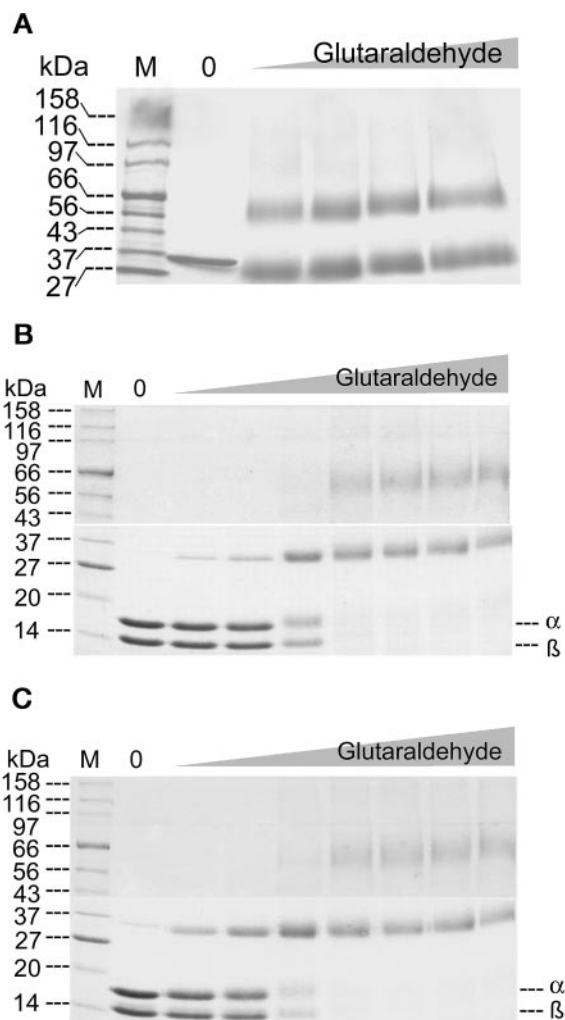


FIG. 2. SDS-PAGE of cross-linked GA precursor and autoproteolyzed amidase. Cross-linking was performed at 0.1 mg/ml (3.1 μ M) of T152A precursor (A), autoproteolyzed wild-type GA (B), and autoproteolyzed T152Cm protein (C), with various amounts of glutaraldehyde at room temperature for 6 h. Two different percentages of acrylamide gels were used in *b* and *c* to separate a wider size range of protein fragments and cross-linked products. Lane *M* is a mixture of molecular weight markers, and lane *0* is a sample treated under the same condition except no cross-linking reagent was added. The rest of the lanes are samples treated with, from left to right, an increasing concentration of glutaraldehyde: 0.1–1% in *a*, and 0.001–1% in *b* and *c*.

GA precursor protein (15) and autoproteolyzed amidase (8), we identified several targets at the dimerization interface for mutagenesis, hoping to weaken or disrupt the dimer formation (Fig. 3A). In the dimers, Val-105 is sequestered out of the solvent to form hydrophobic contacts with its equivalent from the other monomer. Similarly, Ile-186 from each monomer interacts with each other at the dimer interface. In addition, conserved residue Glu-220 forms charge interactions with conserved residue Arg-238 of the adjacent monomer. All of these residues point away from the structural core of the monomer and thus are unlikely to disturb protein packing of each monomer. Furthermore, because these four residues are located on the opposite side of the scissile peptide bond (Fig. 3A), they are not likely to be involved directly in the autoproteolysis. Therefore, replacement of each of these residues was hypothesized to destabilize dimer formation but not to affect the folding of the monomer or to change active site residues.

Four dimer interface mutants were generated to study the effect of mutation at the dimer interface, V105K, I186D, E220K, and R238D. These mutant proteins were also ex-

pressed as MBP fusion proteins by similar protocol published previously (11) for the wild-type and other GA mutants. Purification of GA interface mutants alone proved to be difficult because they were unstable and very sensitive to protease degradation during the process of protein purification, particularly after factor Xa digestion to separate GA mutants from the MBP domain. However, when purified as MBP fusion proteins, these mutants were more stable and thus allowed us to obtain sufficient amounts of proteins for further characterization. Nonetheless, there are still a few minor degradation bands that were eluted together with the MBP-GA full-length protein from a maltose-affinity column (Fig. 3B, lanes 11–18). This indicates these minor degradation products may still retain an intact MBP domain but with a degraded GA mutant domain. This is in contrast to the wild-type GA or other active site mutants that are very stable by the same expression and purification procedure. As shown in Fig. 3B, wild-type GA spontaneously autoproteolyzes into α - and β -subunits during protein purification (lane 2). The T152C mutant also partially autoproteolyzes (lane 3) during the protein purification, resulting in the same α - and β -subunits as the wild-type GA. Furthermore, it has been shown that autoproteolysis of T152C mutant can be accelerated by incubation with hydroxylamine (lane 4; see Ref. 11), indicating a thioester intermediate involved in the autoproteolysis of the T152C mutant. Conversely, T152A mutant loses its critical nucleophile for autoproteolysis (lane 5), and hydroxylamine does not have any effect on autoproteolysis of the T152A mutant (lane 6).

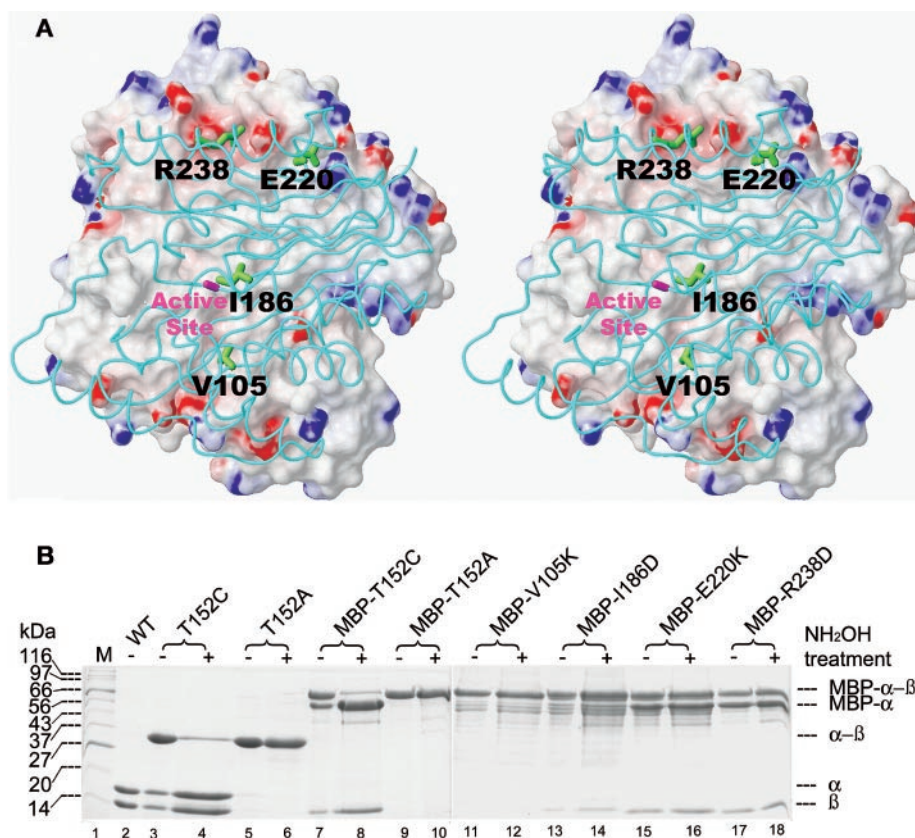
GA retains the same autoproteolytic activity when purified as MBP fusion proteins. MBP-T152C fusion protein partially autoproteolyzes into MBP- α and - β subunits (Fig. 3B, lane 7), and hydroxylamine can also stimulate its autoproteolytic activity (lane 8). MBP-T152A fusion does not autoproteolyze either without or with hydroxylamine (lanes 9 and 10). Thus, expression of GA as MBP fusion proteins does not alter their autoproteolytic activity but can stabilize the dimer interface mutants that are extremely sensitive to protease degradation if isolated as individual GA mutants. We therefore characterized all the dimer interface mutants as MBP fusion proteins and compared them to the controls of MBP-T152A precursor and autoproteolyzed MBP-T152C (MBP-T152Cm) as precursor and mature enzyme, respectively.

Fusion proteins of all four dimer interface mutants are sensitive to degradation during the process of protein purification, but all lose their autoproteolytic activity. The observed degradation products are likely to be clipped at the GA domain because they still can bind to the maltose-affinity column. In addition to affecting the stability of the GA domain, mutations at the dimer interface also disrupt autoproteolytic activity of GA. Unlike the MBP-T152C active site mutant, addition of hydroxylamine does not increase the level of autoproteolysis for any of the dimer interface mutants. The V105K mutant completely loses its autoproteolytic activity in the absence or presence of hydroxylamine (Fig. 3B, lanes 11 and 12). Three other mutants were proteolyzed into two bands that appear to be close to the autoproteolytic products (MBP- α and - β fragments) (Fig. 3B, lanes 13–18). However, these partially proteolyzed enzymes do not have any amidase activity,² suggesting that the clip site could be different from the autoproteolytic site that generates an N-terminal threonine critical for amidase activity. In other words, the processed products might be an act of proteases and not autoproteolysis. It remained a possibility, however, that autoproteolysis did occur in these mutants but with no amidase activity due to some structural changes at the

² C. Guan, unpublished data.

FIG. 3. Structure-based design of mutations to disrupt the dimer interface.

A, stereo view of the dimer interface with the substituted amino acids. One GA precursor monomer is drawn as a molecular surface, colored according to electrostatic potential (blue, positively charged; red, negatively charged), whereas the other monomer is drawn as a cyan polypeptide backbone. In the monomer closer to viewer, the side chains of substituted amino acids (shown in green with the amino acid numbers adjacent to the residues) are on the dimer interface, away from the viewer, whereas the autoproteolytic site (the scissile peptide bond marked in magenta) is on the opposite side of the monomer, toward viewer. The image was made with the program MOLMOL (31) and rendered with Photoshop. **B**, SDS-PAGE analysis of autoproteolysis of wild-type GA, active site mutants (T152C and T152A), and dimer interface mutants (V105K, I186D, E220K, and R238D). The dimer interface mutants are very sensitive to protease degradation and thus could only be partially purified in the context of MBP fusion proteins. Purified protein samples without (-) or with (+) further incubation at 30 °C for 4 h in 10 mM potassium-phosphate buffer, pH 7.4, and 0.5 M hydroxylamine (NH₂OH) were separated on a 15% SDS-acrylamide gel. Lane M is a mixture of molecular weight markers.



active site, although CD spectra show that these mutants retain the wild-type fold (see below). Similar proteolytic trimming near the autoproteolytic site is also observed for the non-autoproteolytic mutants of human GA precursor (18).

Cross-linking Detects No Dimer but Oligomers of Dimer Interface Mutants—Because the mutation sites described above were specifically chosen at the dimer interface, we performed further biochemical assays to assess if these point mutations cause changes in quaternary structure. Cross-linking of MBP fusion proteins indicated that the dimer interface mutations do not form dimers. As a control experiment (Fig. 4A), a fusion protein of MBP-T152A precursor was converted from a monomer band, with an increasing amount of glutaraldehyde, into a new band corresponding to cross-linked dimer, whereas only an uncross-linked band of monomer was observed without glutaraldehyde. In a second control experiment, no cross-linked dimers were observed for the MBP protein itself (Fig. 4B), indicating that the MBP domain does not dimerize in such conditions. Under the same conditions of cross-linking experiments, MBP fusion protein of V105K mutant did not yield a band corresponding to cross-linked dimers. Instead, a significant increase of large size oligomers was retained at the top of gel with a decreased intensity of the monomer band when the concentration of cross-linking reagent was increased (Fig. 4C). Disappearance of the minor degradation bands at high concentration of cross-linking reagent suggests that these degradation products might also exist as oligomers in solution. Similarly, cross-linking of the MBP-I186D mutant also indicated that this mutant tends to form large size oligomers in solutions (Fig. 4D).

Large Size Oligomers Confirmed by Gel Filtration and Sucrose Density Gradient—Large size oligomers of dimer interface mutants were confirmed by gel filtration, to verify that the cross-linking truly reflected the existence of large size oligomers in solution and was not due to interoligomeric cross-

linking. As a control, MBP-T152A precursor was eluted at a volume corresponding to 138 kDa, which approximates the predicted molecular mass of a dimer (Fig. 5A, also see Fig. 1B). However, MBP-I186D mutant was eluted at the peak of the void volume, representing oligomers with sizes of at least several hundred kDa. Similar results were observed for other dimer interface mutants (data not shown).

Sucrose gradient experiments further confirmed the large size oligomers observed in cross-linking and gel filtration (Fig. 5B). At 4 °C, MBP-T152A (75 kDa) precursor yielded a major peak between two reference standards, bovine serum albumin (66 kDa) and γ -globulin (158 kDa), indicating an unusual sedimentation velocity midway between those expected for monomer and dimer, similar to its unusual mobility on a gel filtration column (Fig. 1). Autoproteolyzed fusion protein (MBP-T152Cm) also yielded a major peak near that of the MBP-T152A precursor. In contrast, the majority of both MBP-V105K and MBP-I186D mutant proteins sedimented at the bottom of the gradient, representing species of large size oligomers. No distinct peaks representing dimers were observed for these dimer interface mutants. Continuous trace amount of proteins were detected throughout the sucrose gradient, presumably representing various size oligomers of these dimer interface mutants.

Mutant Oligomers Show Secondary Structure Content Close to the Dimers—To investigate structural features of the large size oligomers observed above, MBP fusion proteins of the dimer interface mutants were analyzed by far-UV CD, and the results were compared with those of the MBP-T152A precursor and MBP-T152Cm mature enzyme (Fig. 6A). The CD spectra showed that the dimer interface mutants retain most of the secondary structure when compared with the dimers of MBP-T152A precursor or MBP-T152Cm mature enzyme. The CD spectrum of the single chain precursor MBP-T152A closely superimposed that of the autoproteolyzed, two-subunit com-

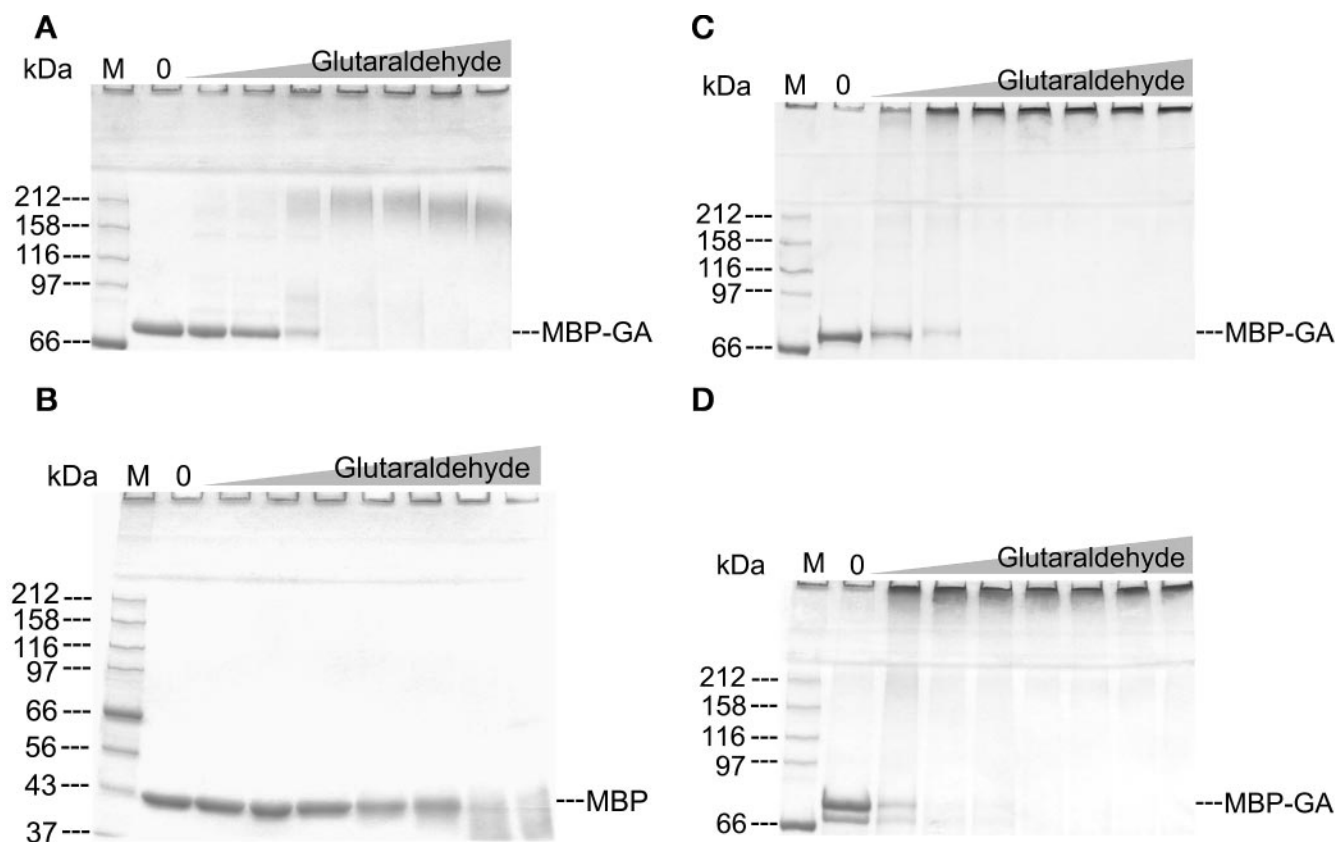


FIG. 4. **SDS-PAGE of cross-linked MBP-T152A precursor and MBP fusion proteins of dimer interface mutants.** Cross-linking was performed at 0.1–0.2 mg/ml (1.3–2.6 μM) of MBP-T152A precursor (A), MBP protein (B), MBP-V105K mutant (C), and MBP-I186D mutant (D), with increasing amounts of glutaraldehyde at room temperature for 6 h. A slightly higher concentration (0.2 mg/ml) of protein samples was used for dimer interface mutants (C and D) to compensate for the co-purified degradation products (see text). Lane M is a mixture of molecular weight markers, and lane 0 is a sample treated under the same condition except no cross-linking reagent was added. Subsequent lanes are samples treated with, from left to right, an increasing concentration of glutaraldehyde from 0.0005–0.05%.

plex of MBP-T152Cm mature enzyme. This is consistent with crystal structures that revealed essentially identical secondary structure contents in both GA forms (8, 15). Interestingly, the CD spectra also showed that the large size oligomers of dimer-disruptive mutants retain substantial amount of intensity from 205 to 250 nm when compared with that of MBP-T152A dimer or dimer of MBP-T152Cm mature enzymes. The largest difference of intensity is around 222 nm where the dimer-disruptive mutants still showed 83% intensity of the native dimers. These results suggest that these high molecular weight oligomers are not denatured protein aggregates. Instead, they could represent higher order oligomeric species of properly folded GA monomers. The differences in CD signals between GA dimers and oligomers of dimer interface mutants might be lessened if the concentrations of the latter were adjusted for the co-purified degradation products (see above and Fig. 3B). Furthermore, the small difference in CD spectra may have also resulted from quaternary and not tertiary structural changes in each monomer (see below).

Differences in the Thermal Stability between Oligomers or Dimers of Precursor and Autoproteolyzed GA—To study thermal stability of dimers and high molecular weight oligomers of the dimer disruptive mutants, the heat unfolding of various GA mutants and MBP fusion proteins was monitored by far-UV CD at 222 nm (Fig. 6, B and C). In neutral 10 mM phosphate buffer solutions containing 2 μM protein, the MBP-T152A precursor unfolds from about 55–60 °C with $T_m = 57.4 \pm 0.5$ °C, whereas the MBP-T152Cm autoproteolyzed protein unfolds from about 58–63 °C with $T_m = 60.3 \pm 0.5$ °C (Fig. 6B), which is 2.9 °C (or 6 times the standard errors) higher than T_m of the MBP-T152A

precursor. Interestingly, both MBP-V105K and MBP-I186D mutants unfold with melting temperature ranges and T_m values almost identical to that of the MBP-T152A precursor, even though these dimer interface mutants are predominantly high molecular weight oligomers. Furthermore, the widths of the single Gaussian function of the differential melting curves $d[\Theta_{220}]/dT$ (inset in Fig. 6B) are nearly identical (about 6 °C), suggesting that unfolding cooperativity is identical among the oligomer of dimer-disruptive mutants and dimer of MBP-T152A precursor. Because the difference in the melting temperatures between the precursor and the autoproteolyzed protein was detected for MBP fusion proteins, we performed additional thermal unfolding studies of isolated GA proteins to assess if the difference in thermal stability resides in the GA domains (Fig. 6C). Similar to the MBP fusion proteins, autoproteolyzed dimers of T152Cm unfolded 3.9 °C higher than precursor dimer of T152A. The wild-type mature protein unfolded at an even higher temperature (more than 6 °C higher than the T_m of the T152A precursor dimer). The difference in melting temperature between the mature T152Cm protein and the mature wild-type GA might be due to some residual amount of T152C protein remaining in the precursor form (see Fig. 3B, lane 4). Thus the apparent melting temperatures of the predominantly mature enzymes of T152C mutant were lowered by this residual precursor. We were unable to separate this residual precursor from the T152C mature form, and we could not make the autoproteolysis of the T152C mutant to 100% completion. Nonetheless, these results indicate that the autoproteolyzed GA dimers (both wild-type and T152Cm mature form) are thermally more stable than the dimer of the T152A

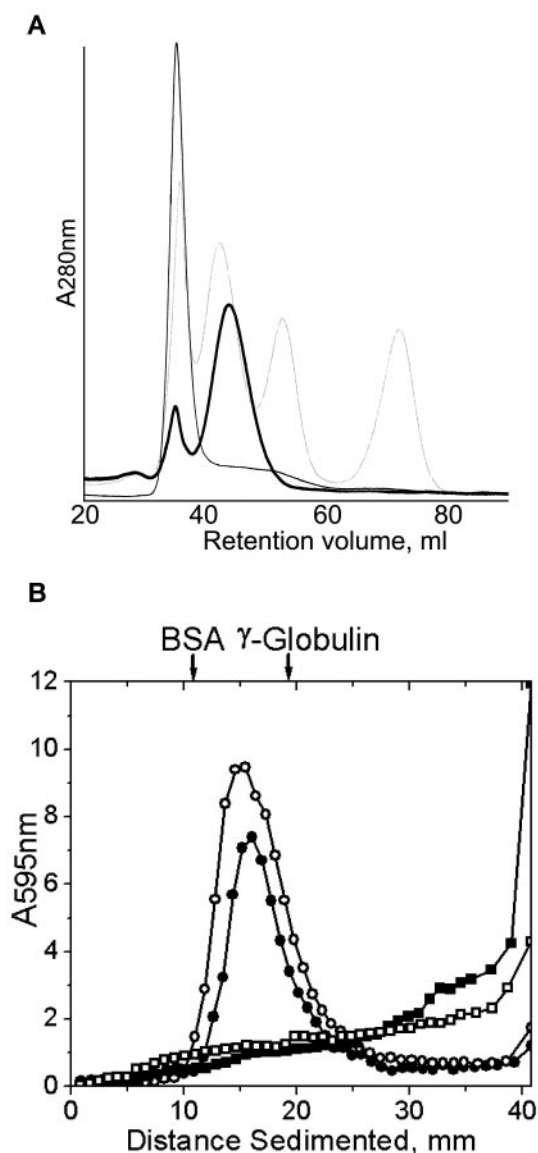


FIG. 5. Characterization of MBP fusion proteins of dimer interface mutants. *A*, gel filtration chromatograms of MBP-GA fusion proteins. *Thick line*, MBP-T152A precursor; *thin line*, MBP-I186D mutant; and *background line*, a mixture of molecular mass standards from *left to right*: bovine thyroglobulin (670 kDa), bovine (BSA) γ -globulin (158 kDa), chicken ovalbumin (44 kDa), and equine myoglobin (17 kDa). Proteins were gel-filtrated in a solution of 10 mM potassium-phosphate buffer, pH 7.4, and 1 mM EDTA, with a flow rate of 0.5 ml/min. *B*, sucrose density gradient profiles of MBP-GA dimers (T152A and T152Cm) and dimer interface mutants (V105K and I186D) at 4 °C for MBP-T152A precursor (●), MBP-T152Cm mature enzyme (○), MBP-V105K mutant (■), and MBP-I186D mutant (□). Sedimentation distances of two reference proteins, γ -globulin (158 kDa) and bovine serum albumin (66 kDa), are indicated by *arrows*. Aliquots (100 μ l) of protein (30 μ M) were layered on 10–30% sucrose gradients and centrifuged at 40,000 rpm for 12 h in a Beckman SW55 Ti rotor. Protein was detected by Bradford assays of a series of 100- μ l fractions taken from the top of the gradients. Sedimentation is depicted from *left to right*.

precursor. On the other hand, the dimeric T152A precursor has a similar thermal stability to the high molecular weight oligomers that are unable to form native dimers and remain in the precursor form. CD studies have shown that the GA precursor has similar secondary structure content to the autoproteolyzed GA. Crystal structure studies have also shown that GA precursor has essentially the same dimer structure as the autoproteolyzed amidase, with an exception of a non-structured link in the precursor between α - and β -subunits (15).

Because this precursor link is on the opposite side of the dimer interface, it cannot explain why the precursor dimer has a lower melting temperature than the autoproteolyzed dimer. One intriguing explanation for the difference in thermal stability is that it is due to stronger monomer-monomer interactions in the autoproteolyzed dimers than in the precursor oligomers (either dimeric or oligomeric) (see below).

DISCUSSION

The data presented here clearly show that GA dimerizes in solution. Gel filtration experiments of MBP-GA fusion proteins suggested that GA, either as a single chain precursor or as an autoproteolyzed amidase, forms dimers in solution. Dimerization was further confirmed by cross-linking experiments. Site-directed mutations at the assumed dimer interface resulted in proteins in which the secondary structure was largely intact but in which the quaternary structure was changed, disrupting dimer formation but forming high molecular weight oligomers.

Previous Reports Reconciled—The contradictory conclusions in previous reports can be attributed to the relatively low resolution of the methods used to separate dimer from monomer, gel filtration chromatography or native gel electrophoresis. By using gel filtration chromatography, GA dimers happen to be eluted in the chromatograms right at the middle between expected fractions of dimers and monomers. In a similar experiment (17), reported dimers of human GA had also been eluted in fractions with much smaller apparent molecular weight (eluted at a 60-kDa fraction whereas the human monomer is 42 kDa). In fact, a single peak eluted at 1.5-fold of monomer size was concluded to be a monomer in one report (11), whereas a similar abnormal elution volume was concluded to be a dimer for human enzyme (17). These results all seem to be due to the compact and non-elongated shape of a GA dimer revealed in crystal structures. In addition to molecular shape and size, the results of sizing chromatography are sensitive to other experimental conditions such as matrix composition, pH, and ionic strength. Interestingly, a dimer interface mutation of human GA precursor (I240D in Ref. 17) equivalent to the bacterial I186D mutant was also found to remain in the precursor form. In the same report (17), a small amount of the precursor of the human dimer interface mutant was found by immunoprecipitation to be eluted in the monomeric but not the dimeric fractions. However, that study did not look into the fractions that could contain large size oligomers of the mutated precursor, as did the bacterial I186D mutant in this study.

Although the dimerization appears to be important for autoproteolysis, the autoproteolysis still could be a first-order reaction. One argument against the significance of GA dimerization in autoproteolysis was that the autoproteolytic reaction follows first-order kinetics (11). This could be reconciled if the dimerization is a prerequisite, but not the rate-limiting, step of the intramolecular autoproteolysis (see below). Because precursors exist predominantly as dimers, dimerization does not appear to be the rate-limiting step of autoproteolysis. Instead, the rate-limiting step appears to be the breaking of the scissile peptide bond (to relieve the conformational constraints). Thus, autoproteolysis would follow a first-order reaction because the concentration of dimer is proportional to the concentration of precursor proteins.

The crystallographic observations are also consistent with our conclusion that GA exists predominantly as dimers in solution. The bacterial GA precursor and autoproteolyzed amidase crystallize in different crystal forms but share the same dimer structure (8, 15, 21). Furthermore, the same dimer structure was also observed for the human GA (7) crystallized in different crystal forms. All of these results are consistent with the notion that this dimer structure is of biological significance.

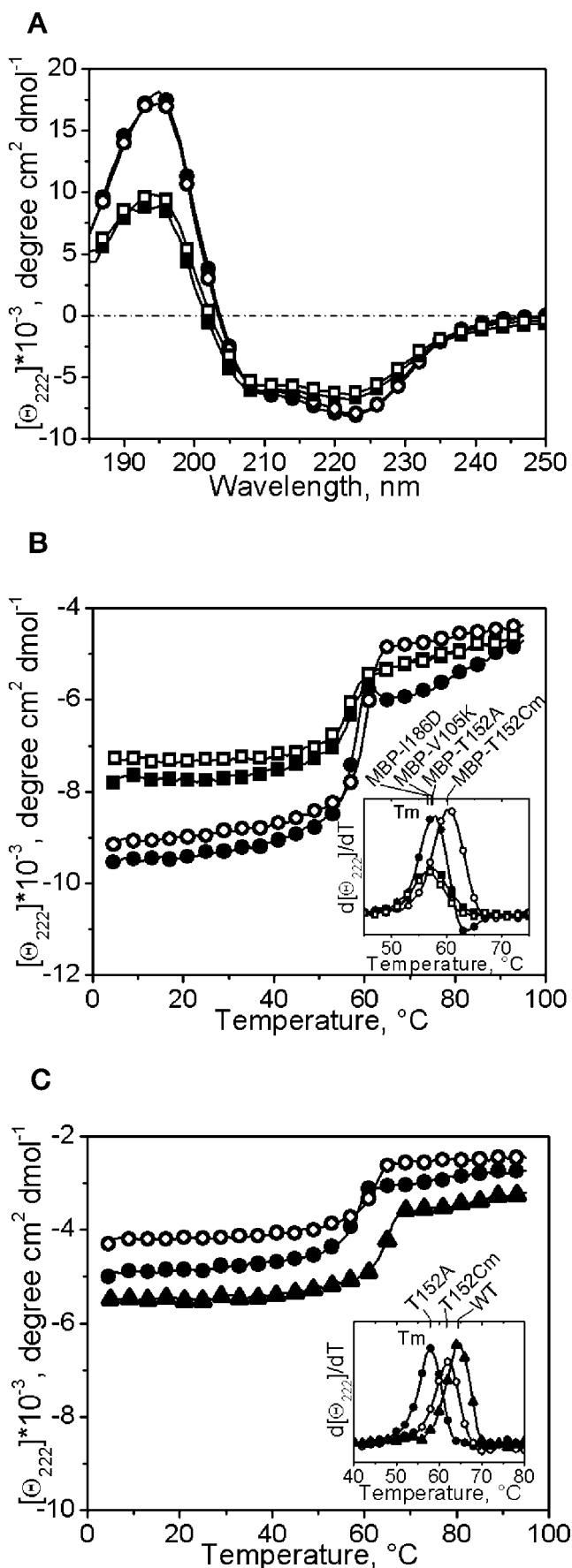


FIG. 6. Far-UV CD spectra of precursor dimer, autoproteolyzed amidase dimer, and dimer-interface mutants. *A*, the spectra were recorded from 2 μM protein solutions in 10 mM potassium-phos-

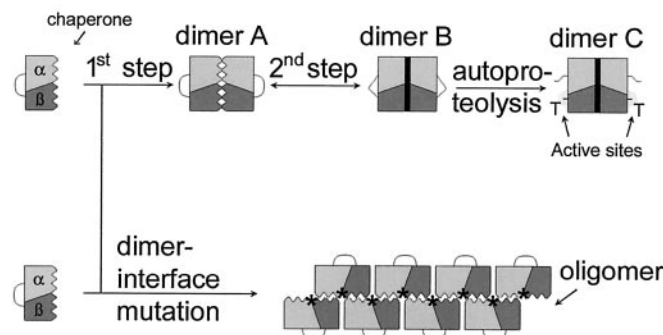


FIG. 7. **Two-step dimerization is essential for autoproteolytic activation of GA amidase.** The α - and β -subunits of GA are initially joined by a loop that is autoproteolyzed to activate the amidase active site. In the first step of dimerization, two molecules of wild-type GA form a dimer (*dimer A*) through an extensive hydrophobic surface from each monomer. This is followed by an equilibrium with *dimer B*, which has stronger dimer interactions but at the expense of creating structural constraints near the scissile peptide bond, as observed in the crystal structures of GA precursors (15). As a result, autoproteolysis is triggered to remove such structural constraints and generate the N-terminal threonines essential for the amidase activity (*dimer C*). Single amino acid substitutions at the dimer interface (indicated by an asterisk) prevent dimer formation but result in oligomerization through similar monomer-monomer interactions as in *dimer A*. However, such oligomerizations are non-productive in generating the structural constraints required to trigger autoproteolysis.

Furthermore, in the crystal structures, the surface interactions in the dimer formation are extensive and mainly involve hydrophobic contacts and hydrogen bonds. Basically, both monomers use the same hydrophobic surface for the dimer formation, reminiscent of hand-shaking. Unless there is a large conformational change as a result of dimerization, it is not likely that the extensive hydrophobic dimer interface observed in the crystals (2485 and 1882 \AA^2 from each monomer of human and bacterial GA, respectively) would be exposed to the solvent as it would in a monomer. The compact and near globular shape of the dimer structure can also explain why the GA behaves differently from the protein size standards that are more irregular in shape.

Prerequisite of Dimerization in Autoproteolysis—A correlation between disruption of dimerization and loss of autoproteolysis indicates that GA dimerization plays an essential role in the intramolecular autoproteolysis. Based on the crystal structures, calculations of the solvent exposure of Val-105, Ile-186, Glu-220, and Arg-238 side chains are 0.8, 0, 4.5, and 21% solvated, respectively, in the dimer *versus* 57, 33, 44, and 48%, respectively, in the monomer, indicating that these residues are largely buried in the dimer but would be considerably exposed as a monomer. Thus substitutions at these positions are likely to affect the dimerization and not the secondary and presumably the tertiary structure of a monomer. In the I186D mutant, the hydrophobic side chain of Ile-186 was substituted with a hydrophilic side chain Asp. This mutant fails to form a dimer but instead oligomerizes into a large size complex (likely larger than hexamers). At the same time, the I186D mutant

phate buffer, pH 7.4, and 1 mM EDTA at 25 $^{\circ}\text{C}$: MBP-T152A (\bullet), MBP-T152Cm (\circ), MBP-V105K (\blacksquare), and MBP-I186D (\square). Following the buffer base-line correction, the spectra were normalized to the protein concentration and are expressed as molar ellipticity. *B*, thermal unfolding of MBP-GA fusion proteins monitored at 222 nm upon heating the sample solutions from 5 to 95 $^{\circ}\text{C}$. Line codings are as in *a*. *Inset*, first derivative $d[\theta]_{222}/dT$ to determine the melting temperature T_m at the centers of the derivative peaks. *C*, thermal unfolding of GA wild-type amidase and mutants, monitored under the same condition as in *B*: autoproteolyzed wild-type GA (\blacktriangle), T152A precursor (\bullet), and autoproteolyzed T152Cm protein (\circ).

also loses the ability to activate its amidase activity by autoproteolysis. In the human GA, an amino acid substitution at the equivalent position (Ile-240) also disrupts the dimer formation of the precursor protein and prevents proteolytic activation of the enzyme (17, 18). Similarly, other dimer interface mutants also fail to dimerize and lose the ability of autoproteolytic activation to form mature amidase. It is possible that these mutations may disturb protein folding and thus prevent autoproteolysis. However, the CD spectra suggest that these mutations do not cause a large change in the secondary structure content. Therefore, the absence of autoproteolytic activation of these mutants is likely due to a disturbance of dimerization and a change in quaternary structure. The fact that the oligomers of dimer interface mutants have similar CD spectra and thermal melting temperature to T152A precursor dimer suggests that similar monomer structure and monomer-monomer interactions are utilized in the precursor dimers and the high molecular weight oligomers. Because these mutations were made on the opposite side of the scissile peptide bond, they are not likely to be directly involved in the autoproteolysis. Therefore, loss of autoproteolysis in the mutant oligomers indicates that a unique structure required to trigger autoproteolysis, presumably a constrained scissile peptide bond as observed in crystal structures, cannot form in the high molecular weight oligomers. In summary, based on data reported here and other evidence in the literature, it appears that dimerization of GA precursor proteins is a prerequisite to trigger autoproteolytic activation of the amidase activity.

Two-step Dimerization Model—With regard to the role of dimerization and the mechanism of GA activation by intramolecular autoproteolysis, we propose a two-step dimerization mechanism preceding GA autoproteolysis (Fig. 7). There are three dimer conformations involved in this model. The initial monomer-monomer interactions mainly involve hydrophobic surfaces from each of two precursor monomers (dimer A). This is followed by a final mesh of the dimer interfaces with a “locking” device (dimer B), such that stronger dimer interactions are achieved but at the expense of creating structural constraints near the scissile peptide bond, as observed in the crystal structures of GA precursors (15). Autoproteolysis would then be triggered to relieve these local constraints without changing the dimer structure, resulting in autoproteolyzed/mature amidase (dimer C). It is intriguing that the van der Waals surface of the dimer interface in crystal structures is relatively flat, except that His-101 from one monomer penetrates into the second monomer and forms hydrogen bonds with the carboxyl group of Glu-207 and the main chain nitrogen of Met-177 (8, 15). It is thus plausible that the intermolecular interactions between His-101 and Glu-207/Met-177 could serve as a locking device in the second step of dimerization to the precise orientation to create structural constraints near the scissile peptide bond.

Wild-type GA autoproteolyzes spontaneously in cells (11). However, if the autoproteolysis was stopped, such as in the T152A precursor or by glycine as reversible inhibitor (15), the activated dimer B with local structural constraints could change through an equilibrium back to the dimer A conformation that has weaker dimer interactions and thus is less thermostable than dimer C. Such an equilibrium between dimers A and B is consistent with our observations that precursors stopped at autocleavage tend to form some large size oligomers (e.g. T152A in Fig. 5A), probably by changing back to dimer A-like conformations. On the other hand, if the first step dimer formation was prohibited, such as by introducing charge repulsion at the dimer interface as in this study, the mutated monomers could still interact with each other through hydrophobic

contacts using the similar non-polar surfaces to form oligomers. This could explain the similar CD spectra and thermal melting temperatures between T152A precursor dimers and oligomers of dimer-disruptive mutants. Nonetheless, such oligomerization of dimer-disruptive mutants is non-productive in generating the structural constraints near the scissile peptide bonds that are required to trigger autoproteolysis.

The two-step dimerization mechanism suggests that T152A precursor will form an equilibrium between dimers A and B, whereas the autoproteolyzed form of T152Cm protein or wild-type GA would exist exclusively in dimer C conformation. Thus the measurement of T_m for T152A precursor is an average of dimers A and B weighted by their percent population. It is not known whether dimer A or B is the predominant form of T152A precursor in solution. Another puzzle is that the crystal structure of precursor dimer is essentially the same as the mature dimer C (15). One intriguing explanation is that only dimer B, not dimer A, is stable enough to crystallize. According to the model, the rate-limiting step of autoproteolysis could be at the autocleavage of the constrained peptide backbone to generate a mature amidase. Therefore, it would help explain why the autoproteolysis is a first-order reaction even though it occurs as a dimer.

A two-step dimerization might be necessary to turn on GA autoproteolysis at the last step to form the native quaternary structure, by an unusual twist at the scissile peptide bond. The same non-polar surface may interact with chaperones during an early stage of GA folding, similar to the interactions in oligomers of dimer-disruptive mutants. Thus if local structural constraints were generated during chaperone-GA interactions, they would either be removed by protein refolding without a productive autoproteolysis or would lead to premature autoproteolysis with non-native structure. The second step dimerization with precise locking device would ensure proper autoproteolysis with native structure. It remains to be determined whether the two-step dimerization mechanism could be extended to autoproteolysis mechanisms of other Ntn hydrolase family members, most of which are found in crystals as oligomeric forms. For example, proteasome from *Saccharomyces cerevisiae* is a 28-oligomer structure consisting of a four-layered barrel structure, with seven unidentical subunits in each layer (28). Penicillin V acylase from *Bacillus sphaericus* is tetrameric (29), whereas glutamine phosphoribosylpyrophosphate amidotransferase from *Escherichia coli* is a dimer (30). More work is required to determine the significance of oligomerization in autoproteolysis of other Ntn hydrolases.

Acknowledgments—We thank Drs. Bullitt and Gursky for critical reading and comments on the manuscript, members of the lab for helpful suggestions, and C. Guan for assistance in protein purification.

REFERENCES

1. Aronson, N. N., Jr., and Kuranda, M. J. (1989) *FASEB J.* **3**, 2615–2622
2. Mononen, I., Fisher, K. J., Kaartinen, V., and Aronson, N. N., Jr. (1993) *FASEB J.* **7**, 1247–1256
3. Tollersrud, O. K., and Aronson, N. N., Jr. (1992) *Biochem. J.* **282**, 891–897
4. Liu, Y., Dunn, G. S., and Aronson, N. N., Jr. (1996) *Glycobiology* **6**, 527–536
5. Tarentino, A. L., and Plummer, T. H., Jr. (1993) *Biochem. Biophys. Res. Commun.* **197**, 179–186
6. Brannigan, J. A., Dodson, G., Duggleby, H. J., Moody, P. C. E., Smith, J. L., Tomchick, D. R., and Murzin, A. G. (1995) *Nature* **378**, 416–419
7. Oinonen, C., Tikkanen, R., Rouvinen, J., and Peltonen, L. (1995) *Nat. Struct. Biol.* **2**, 1102–1108
8. Guo, H.-C., Xu, Q., Buckley, D., and Guan, C. (1998) *J. Biol. Chem.* **273**, 20205–20212
9. Xuan, J., Tarentino, A. L., Grimwood, B. G., Plummer, T. H., Jr., Cui, T., Guan, C., and Van Roey, P. (1998) *Protein Sci.* **7**, 774–781
10. Oinonen, C., and Rouvinen, J. (2000) *Protein Sci.* **9**, 2329–2337
11. Guan, C., Cui, T., Rao, V., Liao, W., Benner, J., Lin, C. L., and Comb, D. (1996) *J. Biol. Chem.* **271**, 1732–1737
12. Tikkanen, R., Riikonen, A., Oinonen, C., Rouvinen, R., and Peltonen, L. (1996) *EMBO J.* **15**, 2954–2960
13. Paulus, H. (2000) *Annu. Rev. Biochem.* **69**, 447–496

14. Perler, F. B., and Adam, E. (2000) *Curr. Opin. Biotechnol.* **11**, 377–383
15. Xu, Q., Buckley, D., Guan, C., and Guo, H.-C. (1999) *Cell* **98**, 651–661
16. Poland, B. W., Xu, M. Q., and Quijcho, F. A. (2000) *J. Biol. Chem.* **275**, 16408–16413
17. Riikonen, A., Rouvinen, J., Tikkanen, R., Julkunen, I., Peltonen, L., and Jalanko, A. (1996) *J. Biol. Chem.* **271**, 21340–21344
18. Saarela, J., Laine, M., Tikkanen, R., Oinonen, C., Jalanko, A., Rouvinen, J., and Peltonen, L. (1998) *J. Biol. Chem.* **273**, 25320–25328
19. Tollersrud, O. K., Heiskanen, T., and Peltonen, L. (1994) *Biochem. J.* **300**, 541–544
20. Kaartinen, V., Williams, J. C., Tomich, J., Yates, J. R., III, Hood, L. E., and Mononen, I. (1991) *J. Biol. Chem.* **266**, 5860–5869
21. Cui, T., Liao, P.-H., Guan, C., and Guo, H.-C. (1999) *Acta Crystallogr. Sect. D Biol. Crystallogr.* **55**, 1961–1964
22. Edelhoch, H. (1967) *Biochemistry* **6**, 1948–1954
23. Martin, R. G., and Ames, B. N. (1961) *J. Biol. Chem.* **236**, 1372–1379
24. John, D. M., and Weeks, K. M. (2000) *Protein Sci.* **9**, 1416–1419
25. Guan, C., Liu, Y., Shao, Y., Cui, T., Liao, W., Ewel, A., Whitaker, R., and Paulus, H. (1998) *J. Biol. Chem.* **273**, 9695–9702
26. Riikonen, A., Tikkanen, R., Jalanko, A., and Peltonen, L. (1995) *J. Biol. Chem.* **270**, 4903–4907
27. Tarentino, A. L., Quinones, G., Hauer, C. R., Changchien, L. M., and Plummer, T. H., Jr. (1995) *Arch. Biochem. Biophys.* **316**, 399–406
28. Groll, M., Ditzel, L., Lowe, J., Stock, D., Bochtler, M., Bartunik, H. D., and Huber, R. (1997) *Nature* **386**, 463–471
29. Suresh, C. G., Pundle, A. V., SivaRaman, H., Rao, K. N., Brannigan, J. A., McVey, C. E., Verma, C. S., Dauter, Z., Dodson, E. J., and Dodson, G. G. (1999) *Nat. Struct. Biol.* **6**, 414–416
30. Muchmore, C. R., Krahn, J. M., Kim, J. H., Zalkin, H., and Smith, J. L. (1998) *Protein Sci.* **7**, 39–51
31. Koradi, R., Billeter, M., and Wuthrich, K. (1996) *J. Mol. Graphics* **14**, 29–32, 51–55